#### **RESEARCH PAPER**



# Investigation of different biogeochemical cover configurations for mitigation of landfill gas emissions: laboratory column experiments

Jyoti K. Chetri<sup>1</sup> · Krishna R. Reddy<sup>1</sup> · Dennis G. Grubb<sup>2</sup>

Received: 17 August 2021 / Accepted: 18 February 2022 © The Author(s), under exclusive licence to Springer-Verlag GmbH Germany, part of Springer Nature 2022

#### **Abstract**

Municipal solid waste (MSW) landfills are a major source of anthropogenic methane ( $CH_4$ ) and carbon dioxide ( $CO_2$ ) emissions, which are also major greenhouse gases. Apart from greenhouse gas emissions, MSW landfills are notorious for odor, and hydrogen sulfide (H<sub>2</sub>S) is a major contributor of odor in landfills. Recent studies have shown promise with biochar-amended soil covers to mitigate landfill CH<sub>4</sub> emissions by enhancing microbial CH<sub>4</sub> oxidation; however, mitigating only CH<sub>4</sub> does not wholly resolve fugitive emissions as landfill gas (LFG) comprise of almost same proportion of CO<sub>2</sub> as CH<sub>4</sub>. Also, H<sub>2</sub>S has very low odor threshold and numerous health risks. This study explores a novel biogeochemical MSW landfill cover integrating basic oxygen furnace (BOF) slag and biochar-amended soil to mitigate CH<sub>4</sub>, CO<sub>2</sub> and H<sub>2</sub>S simultaneously from LFG. In this regard, column studies were carried out simulating four cover profiles: 1) soil control (column 1); 2) combination of BOF slag layer and 10% (by weight) biochar-amended soil layer (column 2); 3) combination of BOF slag layer and 5% (by weight) methanotrophically activated biochar-amended soil layer (column 3); and 4) combination of mixture of sand and BOF slag layer and 10% (by weight) methanotrophically activated biochar-amended soil layer (column 4). The cover profiles were exposed to simulated LFG (48.25% CH<sub>4</sub>, 50% CO<sub>2</sub> and 1.75% H<sub>2</sub>S) at an average flux rate of 130 g CH<sub>4</sub>/m<sup>2</sup>-day. Terminal batch assays were conducted on the soil and biochar-amended soil samples obtained from various depths after exhumation from the columns to evaluate potential CH<sub>4</sub> oxidation rates. Carbonate content tests and batch tests were conducted to evaluate carbonation potential of the BOF slag. The overall gas removal efficiencies of the cover profiles were in the order of column 3 > column 2 > column 4 > column 1. The CH<sub>4</sub> oxidation rates were the highest in the 5% activated biochar-amended soil at 143 μg CH<sub>4</sub>/g-day or 100 μg CH<sub>4</sub>/g-day above soil control. Higher CH<sub>4</sub> oxidation potential was associated with high moisture retention and biochar content. The BOF slag showed a maximum CO2 removal of 145 mg CO2/g BOF slag during column operation. Carbonation of BOF slag did not impede oxygen intrusion into the underlying biochar-amended soil layer and its CH<sub>4</sub> oxidation efficiency. Overall, biogeochemical cover provides a holistic and sustainable solution to fugitive landfill emissions.

Keywords Activated biochar · Biochar · Biogeochemical cover · BOF slag · Carbonation · Methane oxidation

Jyoti K. Chetri jkc4@uic.edu

Dennis G. Grubb dggrubbphdpe@gmail.com

Published online: 19 March 2022

Department of Civil, Materials, and Environmental Engineering, University of Illinois at Chicago, 842 West Taylor Street, Chicago, IL 60607, USA Fugacity LLC, 324 Broadway Ave, West Cape May, NJ 08204, USA



#### 1 Introduction

Methane (CH<sub>4</sub>) emission from municipal solid waste (MSW) landfills has been an increasing cause of concern across the globe as CH<sub>4</sub> is a highly potent greenhouse gas (GHG) with global warming potential (GWP) of 28-36 over a 100-year period [21, 43]. MSW landfills are the third largest source of anthropogenic CH<sub>4</sub> emissions in the USA, which accounted for nearly 15.1 percent of these emissions in 2019 [43]. In addition to CH<sub>4</sub>, MSW landfills emit other gases including carbon dioxide (CO<sub>2</sub>), hydrogen sulfide (H<sub>2</sub>S) and some non-methane organic compounds (NMOCs). In recent years, studies have shown microbially mediated CH<sub>4</sub> oxidation can mitigate CH<sub>4</sub> emissions from new or old landfills by providing a well-designed landfill cover and engineered biocover system [19]. Biocovers are mainly composed of organic-rich materials such as composts and peats, either alone or amended with landfill cover soil, which can support and promote microbial growth and CH<sub>4</sub> oxidation [18, 40]. However, some organic amendments like compost suffer from issues of degradation in the long term reducing the efficiency of the biocover to mitigate CH<sub>4</sub> [40]. Hence, in recent years, biochar has gained prominence as an organic amendment to landfill cover soil due to its inertness, long-term stability, high moisture retention and gas adsorption potential [40, 48, 50]. Biochar is a solid carbonaceous product derived from biomass (waste) via thermochemical processes such as pyrolysis and gasification [47]. Recent studies have shown biochar amendment improves physicochemical properties of landfill cover soil, improves gas flow, enhances microbial colonization and growth, and ultimately enhances CH<sub>4</sub> oxidation efficiency and rates [34, 49]. Methane oxidation is broadly attributed to methanotrophs, which are part of larger bacterial group named methylotrophs [18, 48]. In recent batch incubation studies, methanotrophic bacterial culture consortium was used to microbially activate biochar prior to amending landfill cover soil to enhance microbial activity in biochar [17, 31]. The activated biochar showed significantly higher CH<sub>4</sub> oxidation rates than the non-amended biochar [31].

Methane, being a highly explosive gas, garners the attention from the operators as well as the regulatory agencies. LFG is also comprised of other environmentally harmful gases such as CO<sub>2</sub> and H<sub>2</sub>S. Carbon dioxide is not only emitted from the waste mass but also during CH<sub>4</sub> oxidation (Eq. 1) increasing the overall CO<sub>2</sub> emissions from the landfill cover. Carbon dioxide is a major GHG, and H<sub>2</sub>S is a highly odorous and toxic gas. H<sub>2</sub>S has very low odor threshold, and long-term low-level exposures may lead to chronic health effects as well as short-term

exposure to high levels may lead to acute health risks, which may be lethal in severe cases [28].

$$CH_4 + O_2 = CO_2 + H_2O$$
 (1)

Some studies have demonstrated potential in biocovers to remove both CH<sub>4</sub> and odor [20, 24, 25, 46]. However, the CO<sub>2</sub> emissions remains a challenge. The increasing global warming and climate change events have necessitated the global communities to take steps to curb these GHG emissions and protect the environment.

Mineral carbonation has emerged as a potential technique to reduce CO<sub>2</sub> emissions [20]. In this process, calcium- or magnesium-containing minerals react with CO<sub>2</sub> and are converted into their respective thermodynamically stable carbonates. In recent years, extensive studies have explored accelerated mineral carbonation techniques using industrial wastes and residues such as steel slags and fly ashes, which are alkaline and rich in calcium [20]. In this regard, basic oxygen furnace (BOF) slag is preferred because of its high residual lime content versus other slags. BOF slag showed promising CO<sub>2</sub> sequestration from simulated LFG in our previous studies [13, 36-38] and significant potential to remove H<sub>2</sub>S because its calcium and iron phases react with CO<sub>2</sub> and H<sub>2</sub>S, respectively [14]. Major calcium-containing minerals include free lime (CaO), portlandite [Ca(OH)<sub>2</sub>] and larnite (Ca<sub>2</sub>SiO<sub>4</sub>), which can readily react with CO<sub>2</sub> forming stable carbonates, as well as iron oxides (FeO, Fe2O3) which react with H2S forming iron sulfides [14].

Although biocovers and steel slags possess significant potential to mitigate CH<sub>4</sub>, CO<sub>2</sub> and H<sub>2</sub>S individually, no study has explored simultaneous removal of all these three major components of LFG in one cover system. Recently, a novel biogeochemical cover was proposed, which combines biochar-amended soil and BOF slag systems to simultaneously mitigate CH<sub>4</sub>, CO<sub>2</sub> and H<sub>2</sub>S [13, 32, 33]. Biochar-amended soil can mitigate CH<sub>4</sub> emissions by enhancing microbial CH<sub>4</sub> oxidation and BOF steel slag can mitigate CO<sub>2</sub> and H<sub>2</sub>S through carbonation and sulfidation reactions. Removal of CH<sub>4</sub> by biochar-amended soil, and CO<sub>2</sub> and H<sub>2</sub>S by BOF steel slag have been investigated extensively through batch incubations and small column tests [14, 36, 48, 49]. However, not much is known about how the combination of biochar-amended soil and BOF slag will perform under simulated LFG conditions. In addition, it is crucial to optimize the biogeochemical cover profile to maximize the LFG removal potential under LFG flow conditions. Hence, this study presents column studies simulating various biogeochemical cover profiles under simulated LFG flow conditions to evaluate the optimal biogeochemical profile and understand the physical conditions needed for optimum gas removal efficiency.



In this regard, four cover profiles were tested in column reactors: 1) soil control; 2) 10% (w/w) biochar-amended soil with overlying BOF slag layer; 3) 5% methanotrophically activated biochar-amended soil with overlying BOF slag layer; and 4) 10% methanotrophically activated biochar-amended soil with BOF slag and sand mixed layer. The main objectives of column experiments were to: 1) evaluate the overall CH<sub>4</sub>, CO<sub>2</sub> and H<sub>2</sub>S removal potential of the biogeochemical cover; 2) compare the CH<sub>4</sub> oxidation rates in activated and non-activated biochar-amended soils and soil control in column reactor; and 3) investigate the effect of providing slag layer over biochar-amended soil layer on gas flow and microbial CH<sub>4</sub> oxidation.

#### 2 Materials and methods

#### 2.1 Characterization of cover materials

Four different materials were used in setting up the test cover profiles (soil, biochar, sand and BOF slag). Landfill cover soil was obtained from intermediate cover of Zion Landfill, Zion (Illinois, USA). A commercially produced pinewood-derived biochar was obtained from Chip Energy, Goodfield (Illinois, USA). BOF slag was obtained from the Arcelor Mittal Steel Plant, Indiana Harbor East, East Chicago (Indiana, USA) in a freshly crushed and dried form with a top sieve size of 10 mm (3/8 in). "Three River"

sand was obtained from a regional quarry (Beloit, WI, USA), which was characterized as a poorly graded sand (SP) by USCS [2]. The individual cover materials were characterized for their physical and chemical properties using the ASTM procedures summarized in Table 1. Hydraulic conductivity of landfill cover soil was determined using flexible wall permeameter, whereas each individual material was tested using constant head permeameter. The pH was determined using a Thermo Scientific Orion 0720A7 pH meter (Fisher Scientific, UK).

## 2.2 Column experiment setup

Four plexiglass columns of internal diameter 18.40 cm and height 100 cm were constructed to test four different cover profiles. Each column had a flanged top and bottom with caps secured with screws and sealed with rubber O-rings. Columns were operated in an upflow mode, wherein the LFG was injected into manifold outfitted with a pressure gauge (flowmeter) and sampling ports for each column. The effluent manifold was outfitted with air and a humidification chamber to simulate atmospheric conditions above the cap and gradient for oxygen flow downward into the cap as shown in Fig. 1. The gas sampling ports were also provided vertically along the height of the column at an interval of 10 cm in the lower 50 cm of the column. The outlets were provided in each column to divert the headspace

Table 1 Characteristics of the cover components tested in the column experiments

Properties	ASTM method	Soil	Biochar*	Sand	BOF slag**
Specific gravity	D854 [10]	2.68	0.65	2.65	3.34
Organic content/LOI (%)	D2974 [3]	5.80	96.71	0.6	1.94
pН	D4972 [7]	7.6	6.5	7.8	12.4
Grain size distribution	D6913/6913 M [9]	3.7	45	0.1	0
Gravel (%)		14.4	54	99.7	86.4
Sand (%)		81.9	1	0.2	13.6
Fines (%)					
$D_{50} \text{ (mm)}$		0.009	4.3	2.1	0.82
$C_c$		_	0.82	1.04	29.17
$C_u$		_	2.42	4.83	0.72
Atterberg Limits	D4318 [5]	39	Non-Plastic	Non-Plastic	Non-Plastic
Liquid limit (%)		22	_	_	
Plastic limit (%)		17	_	_	
Plasticity index (%)					
USCS classification	D2487 [2]	CL	SP	SP	SM
Water-holding capacity (% w/w)	D2980 [4]	43.4	51.6	_	29.6
Hydraulic conductivity (cm/s)	D5084 [1]/D2434 [8]	$5 \times 10^{-8}$	$4 \times 10^{-3}$	$7\times10^{-3}$	$3\times10^{-3}$

<sup>\*</sup>part of data presented in Reddy et al. [36]; \*\* part of data presented in Chetri et al. [14]



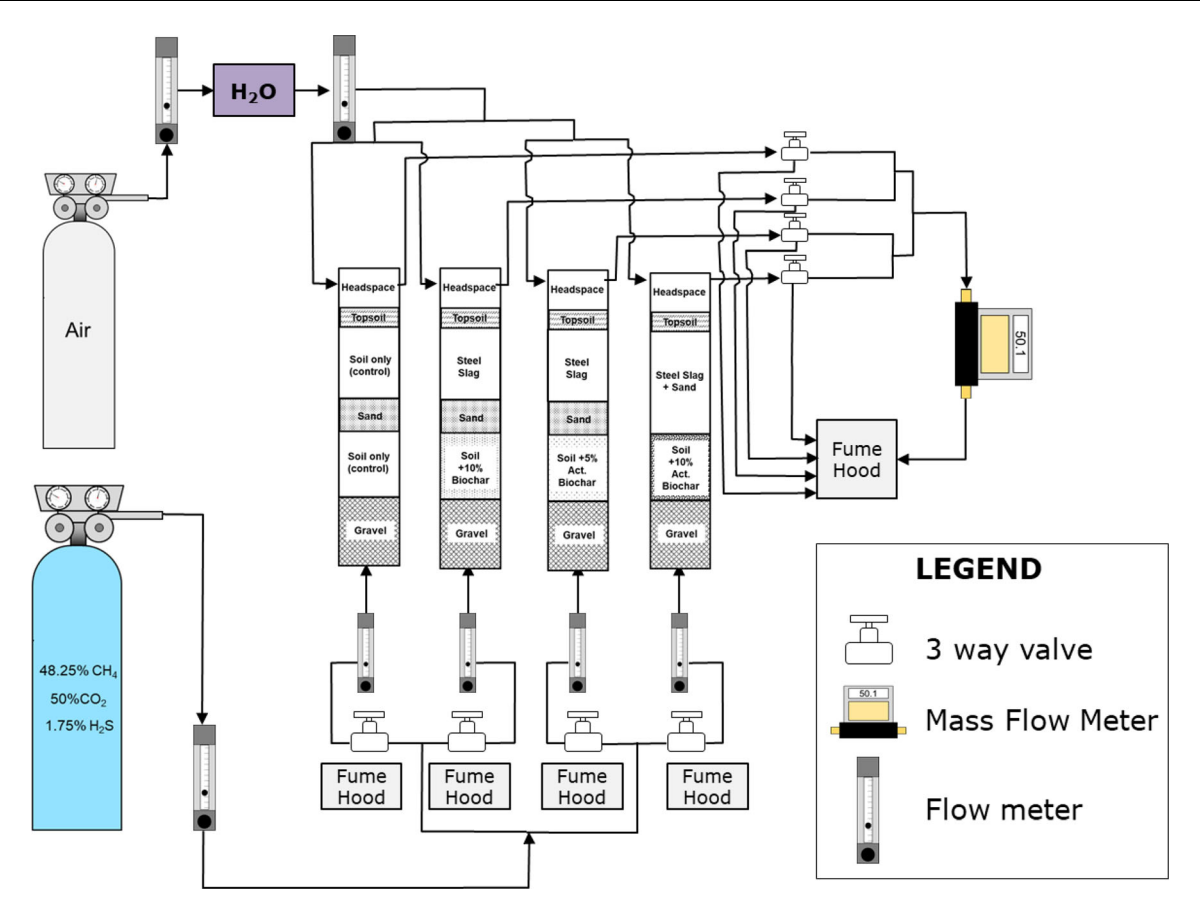


Fig. 1 Schematic of column test setup

gas to the flowmeter and then to the fume hood. The columns were set up and operated in room temperature (23  $\pm$  2  $^{\circ}\text{C}$ ).

The cover materials used for various profiles comprised of landfill cover soil, biochar, sand, and BOF steel slag (Table 1). The methanotrophic bacterial consortium was prepared following the procedure mentioned in Rai et al. [31] and Reddy et al. [35]. Biochar was activated by soaking biochar pellets in consortium. The target moisture content for the biologic layer was 15% based on our previous studies [49] and 10% for BOF slag and BOF slag + sand layers [13]. The layers were placed in 5-cm lifts with light compaction. The layer properties are shown in Table 2. The base of each column was packed with pea gravel (G) to a depth of 25 cm to promote uniform gas flowing from inlet. Above this, a 20-cm biologic layer was installed having various compositions summarized in Fig. 2. Column 1 or control column used a 20-cm-thick landfill cover soil (CS) followed by a 10-cm-thick sand lens (S) to serve as a capillary break to the uppermost 25-cm-thick layer of CS media. Column 2 used landfill cover soil amended with 10% (w/w) of biochar (B10) as the biologic layer and the same capillary break media. This was followed by 20-cm-thick layer of BOF steel slag (SS) and a 5-cm-thick CS layer. The purpose of the BOF slag layer was to trap  $CO_2$  and  $H_2S$ . Column 3 was the same, but the biologic layer was CS with 5% (w/w) of biochar activated with a methane-oxidizing bacterial (MOB) consortium (AB5). Column 4 contained 20 cm of CS with 10% (w/w) activated biochar as a biologic layer (AB10) followed by a 30 cm thick, 2:1 (v/v) mixture of BOF slag and sand (SS-S) created to prevent pore clogging due to carbonation in the long term. A 5-cm-thick CS layer separated the SS-S layer from the effluent part (headspace).

The main function of biologic layer in each column was to oxidize CH<sub>4</sub> through microbial activity. In the columns 2–4, biochar amendment to landfill cover soil at varying proportions was tested to evaluate the effectiveness over landfill cover soil alone in oxidizing landfill CH<sub>4</sub>. The biochar proportion of 5 and 10% were tested to optimize the usage of biochar. Similarly, methanotrophically activated biochar was used in columns 3 and 4 to expedite the microbial oxidation process as adding biochar to the landfill cover soil may extend the acclimation time for microbes. The sand layer above the biologic layer served as a gas distribution layer or capillary break layer for the overlying BOF slag layer. In columns 2 and 3, BOF slag was used as a CO<sub>2</sub> and H<sub>2</sub>S removing layer. In column 4,



Table 2 Physical properties of the cover profiles during setup

Layer	Description	Column					
(bottom to top)		Column 1	Column 2	Column 3	Column 4		
Layer 1	(5 cm lifts, light tamping, 25 blows ea.)						
(20 cm thick)	Bulk density (g/cm <sup>3</sup> )	1.53	1.37	1.51	1.25		
	Dry density (g/cm <sup>3</sup> )	1.31	1.18	1.31	1.08		
	Total porosity (%)	49	52	47	56		
	Air-filled porosity (%)	27	32	27	39		
	Water- filled porosity (%)	22	20	20	17		
	Initial moisture (%w/w)	16.6	16	15.3	15.7		
Layer 2	Loosely placed (Air pluviated)						
(10 cm thick)	Bulk density (g/cm <sup>3</sup> )	1.80	1.80	1.73			
Layer 3 (20 cm thick)	(5 cm lifts, light tamping, 25 blows ea. for soil and 15 blows ea. for slag)						
	Bulk density (g/cm <sup>3</sup> )	1.50	1.73	1.73	1.78		
	Total porosity (%)	52	53	53	52		
	Moisture content (%w/w)	15.43	10.37	10.50	9.84		
Layer 4	(5 cm lift, light tamping, 25 blows ea.)						
(5 cm thick)	Bulk density (g/cm <sup>3</sup> )	1.50	1.54	1.65	1.50		
	Dry density (g/cm <sup>3</sup> )	1.30	1.33	1.44	1.30		
	Total porosity (%)	51	50	46	51		
	Initial moisture (%w/w)	15.43	15.58	14.62	15.23		

BOF slag was mixed with the sand to increase the porosity and reduce any potential pore clogging from carbonation of BOF slag. A soil layer was used on the top of BOF slag in columns 2 to 4 to serve as a vegetative layer or an erosion protection layer.

In terms of column operation, the biologic layer was placed first in each column and preincubated under dynamic gas flow conditions to understand the microbial community response to changing LFG conditions. The results are summarized in our recent study [15]. The layers above biologic layers were placed as a continuation of the column studies shown in Chetri et al. [15] to further assess the effect of overlying BOF slag layers on the microbial community dynamics in addition to assessing overall performance of biogeochemical cover profiles. After column packing was completed, the simulated LFG (48.25% CH<sub>4</sub>, 50% CO<sub>2</sub> and 1.75% H<sub>2</sub>S) was injected at an average influent flux rate of 130 gCH<sub>4</sub> /m<sup>2</sup>-day for around 36 days. The chosen influent flux rate represents the average CH<sub>4</sub> flux rates typically observed in an active MSW landfill [49].

## 2.3 Gas analyses

Gas samples were collected 3–4 times a week from each sampling port installed along the depth and headspace of each column using a 1-mL luer lock-syringe. The gas was then analyzed using SRI 9300 gas chromatography (GC) machine (SRI Instruments, Torrance, California, USA) equipped with thermal conductivity detector (TCD) for the detection of CH<sub>4</sub> and CO<sub>2</sub> (detection limit of 500 ppm) and flame ionization/flame photometric detector (FID/FPD) with a detection limit of 1 ppm (parts per million) for detection of H<sub>2</sub>S. For the measurement of oxygen (O<sub>2</sub>), the carrier gas was switched to nitrogen from helium. The GC was calibrated with standards prior to gas concentration measurement each time.

# 2.4 Column exhumation and terminal characterization

After the LFG supply was terminated, all solids were exhumed and analyzed. Discrete samples were obtained from various depths (Table 3) and analyzed for moisture content (MC), organic content/loss on ignition (OC/LOI), and pH according to the methods shown in Table 1. Additionally, carbonate content tests were performed on each sample in accordance with ASTM [6]. Carbonated BOF slag samples and BOF slag + sand samples were also analyzed by scanning electron microscopy (SEM) using JEOL JSM-IT500HR high-resolution scanning microscope operated at 5.0 kV with a Secondary Electron detector (SED) for imaging. EDS analysis (energy-dispersive spectrometry) was performed for elemental information using Ultim Max, Oxford X-ray energy-dispersive spectrometer operated at @ 20 kV OR 30 kV. Total sulfur



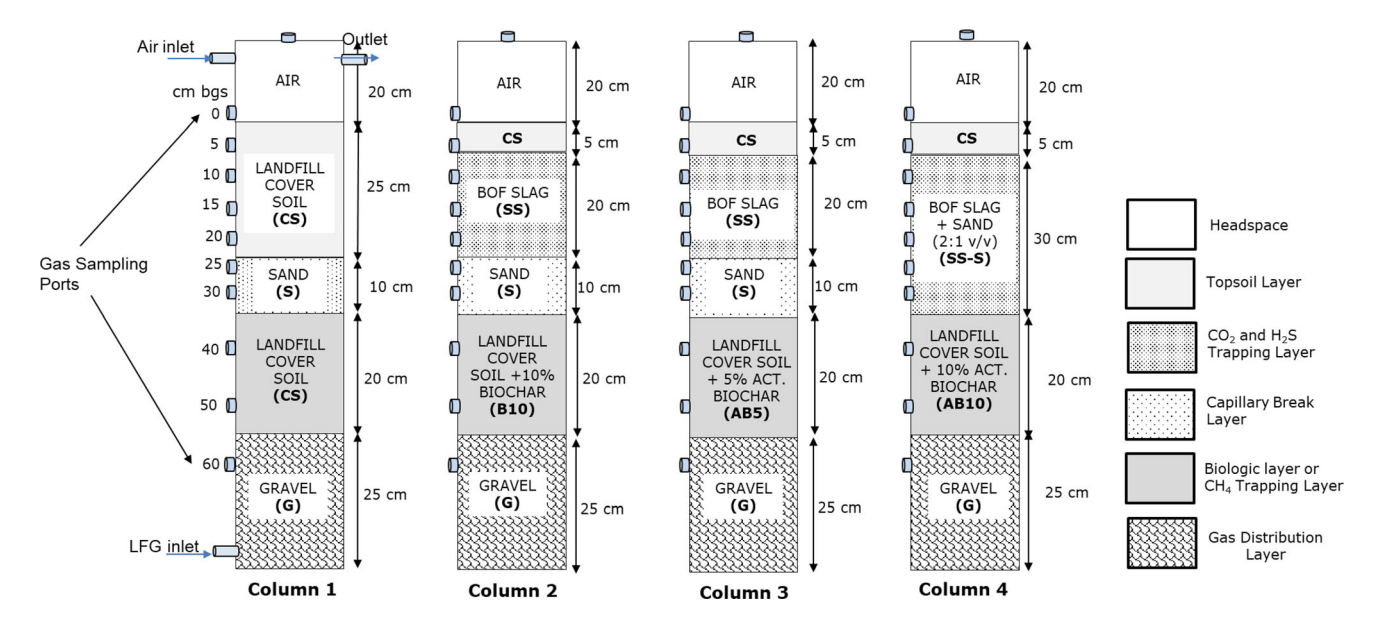
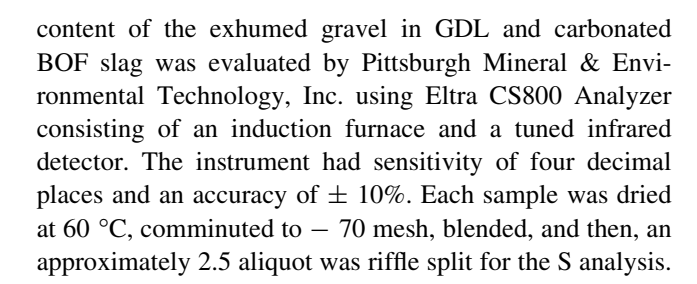


Fig. 2 Schematic of cover configurations tested during column incubation

Table 3 Properties of exhumed column media

	Depth (cm)	MC (%)	OC/LOI (%)	pН
Column 1	10	15.9	3.5	7.9
	15	15.7	3.9	7.8
	20	16.0	3.2	7.8
	40	7.8	5.1	7.6
	45	8.4	4.9	7.6
	50	8.8	5.4	7.7
Column 2	10	10.0	1.7	11.8
	15	9.3	1.8	11.8
	25	10.3	1.9	11.9
	40	10.4	12.8	7.7
	45	8.3	12.5	7.8
	50	10.4	13.1	7.5
Column 3	10	9.3	2.3	10.6
	15	9.2	2.4	11.5
	25	9.1	2.3	11.9
	40	12.5	9.5	7.5
	45	12.7	10.1	7.4
	50	12.8	9.7	7.5
Column 4	10	9.5	1.3	12.1
	15	9.6	1.4	12.1
	25	9.5	1.2	12.1
	30	10.3	1.3	12.1
	40	11.8	16.9	7.9
	45	11.9	12.6	7.9
	50	11.7	11.1	8.0

Sample locations shown on the schematic on the right side *MC* Moisture content, *OC* Organic content, *LOI* Loss on ignition



# 2.5 Terminal batch tests

Freshly exhumed samples from the uppermost CS [5 cm below ground surface (bgs)] and three locations in each bottom biologic layer (40 cm, 45 cm, and 50 cm depth referred to as top, middle and bottom, respectively henceforth) were subjected to batch incubations to determine the ongoing CH<sub>4</sub> oxidation potential of each medium. For the microbial batch incubations, 10 g of exhumed sample was added to a 125-mL glass serum vial and sealed hermetically with butyl rubber septa and aluminum crimps. About 20 mL of air was removed from each vial and replaced with same volume of 50% (v/v) CH<sub>4</sub> / 50% (v/v) CO<sub>2</sub> mixture. The headspace CH<sub>4</sub> and CO<sub>2</sub> concentrations were regularly monitored for one week. CH<sub>4</sub> oxidation rates were determined from the linear regression of CH<sub>4</sub> concentration vs time plot following zero-order kinetics [23, 48]. Batch tests were performed in triplicate.

In addition, a carbonated slag sample extracted from column 3 (sample taken at bottommost part of slag layer or 20 cm from top of SS layer) was subjected to batch test to evaluate residual carbonation capacity of the slag. A batch test was performed using the procedure outlined by Chetri et al. [14]. Briefly, 1 g of the carbonated slag sample was



taken in a 125-mL glass vial and purged with a mixture of 50% (v/v) CH<sub>4</sub> /CO<sub>2</sub>. The vials were then sealed immediately with butyl rubber septa and secured with aluminum crimps. The headspace gas concentrations were monitored over time to evaluate residual carbonation potential of the carbonated slag.

#### 3 Results and discussions

# 3.1 Material characterization before column incubation

The properties of the individual cover substrates are summarized in Table 1. The CS had high percentage of fines. Biochar was in the form of pellets, and hence, the fines content was low. Similarly, the sand (S) also had very low fines content (< 1%). BOF slag had approximately 12% fines (non-plastic). The mean particle size  $(D_{50})$  of biochar was the highest followed by sand and BOF slag. Biochar is known to have high absorption capacity [39, 41], which is reflected in the high water holding capacity ( $\sim 52\%$ ). The landfill cover soil also had relatively higher water holding capacity (~ 44%). Biochar and BOF slag both had permeabilities similar to the sand. However, the permeabilities may vary depending on the gradation of the individual material. Biochar is a carbonaceous material derived from biomass and hence possesses very high OC (97%). CS also had considerably higher OC, which may be due to the microbial biomass. The CS had slightly alkaline pH (7.6), whereas biochar was slightly acidic (pH 6.5). BOF slag was strongly alkaline (pH 12.4) owing to the residual lime content and reactive silicates [14].

The physical properties of each layer are summarized in Table 2. Biochar resulted in lower densities and higher porosities in biochar-amended media than CS in column 1 under similar compactive efforts, which is attributed to the low specific gravity (Table 1) and highly porous structure of the biochar [50]. The sand layer was loosely placed in dry state to facilitate uniform gas distribution in the overlying layers in each column and to serve as capillary break. The BOF slag layers were also lightly compacted; however, the resultant bulk densities were much higher as expected. The total porosities were comparable in CS, SS and SS-S media.

# 3.2 Gas concentration profiles

The gas profiles can be used primarily for qualitative estimation of potential CH<sub>4</sub>, CO<sub>2</sub> and H<sub>2</sub>S removal activity of the cover systems, as there are other several phenomena occurring such as diffusion, advection, dilution, and absorption, which makes the quantification process more

complex [16, 42]. The average CH<sub>4</sub>, CO<sub>2</sub>, and O<sub>2</sub> profiles in each capping system during column operation are shown in Fig. 3. Hydrogen sulfide is not shown as it was completely absorbed in the base gravel layer (inlet) and remained undetected throughout the column operation period. Oxygen penetrated through the entire depth of the cover system, implying that the BOF slag layer did not obstruct O<sub>2</sub>, thus enabling CH<sub>4</sub> oxidation in the biologic layer below. The gas profiles show CO<sub>2</sub> concentrations higher than CH<sub>4</sub> in each biologic layer. The elevated CO<sub>2</sub> concentrations in the biologic layers are an evidence of occurrence of CH<sub>4</sub> oxidation as CO<sub>2</sub> is produced in microbial CH<sub>4</sub> oxidation [49]. The ratio of CO<sub>2</sub> to CH<sub>4</sub> (CO<sub>2</sub>/CH<sub>4</sub>) was higher (1.2–1.4) than the initial gas ratio fed to the columns (1.03) at the interface of gas distribution layer and biologic layer. This could be an indication that CH<sub>4</sub> oxidation was occurring even in the gas distribution layer [30, 48] or could be due to differences in the diffusion coefficient of CO<sub>2</sub> (1.61  $\times$  10<sup>-5</sup> m<sup>2</sup> s<sup>-1</sup> at 22 °C) and CH<sub>4</sub>  $(2.12 \times 10^{-5} \text{ m}^2 \text{ s}^{-1} \text{ at } 22 \text{ °C})$  in air [16]. The control column (column 1) showed a gradual decrease in the concentrations of both CH<sub>4</sub> and CO<sub>2</sub> toward the top of the column, whereas the CO<sub>2</sub> concentrations were greater than CH<sub>4</sub> throughout (Fig. 3a) perhaps due to CH<sub>4</sub> oxidation in CS media. In column 2, the CH<sub>4</sub> concentration was reduced in the B10 layer and CO<sub>2</sub> concentration showed steep decline while transitioning into the overlying SS media and then complete removal (Fig. 3b). In column 3, the CO<sub>2</sub> concentration was elevated in the AB5 layer likely due to CH<sub>4</sub> oxidation, which was then completely removed by the SS layer (Fig. 3c). Similarly, in column 4, CH<sub>4</sub> was oxidized in the AB10 layer releasing CO<sub>2</sub> consistent to biologic layers in other columns; however, the SS-S layer was not very effective in sequestering CO<sub>2</sub> (Fig. 3d) despite the same overall SS content. It is likely that SS-S layer had formed preferential flow paths reducing the residential time and carbonation of SS. A rapid decrease in O2 concentration was observed in the biologic layer in all four columns, which is attributed to the consumption of O<sub>2</sub> during microbial CH<sub>4</sub> oxidation.

Figure 4a, c shows headspace concentrations of  $CH_4$  and  $CO_2$  in each column during incubation.  $H_2S$  concentrations remained undetectable in the headspace throughout the experiment due to reaction/adsorption in underlying layers mainly gravel as darkening of gravel was evidenced during LFG exposure. The darkening of the gravel suggests precipitation of the sulfide from reaction with metal salts possibly present in the gravel as per the reaction given in Eq. 2.

$$M^{++} + H_2S = MS + 2H^+$$
 (2)

Wohlers and Feldstein [45] reported darkening of the exterior paints due to exposure to  $H_2S$ , which was



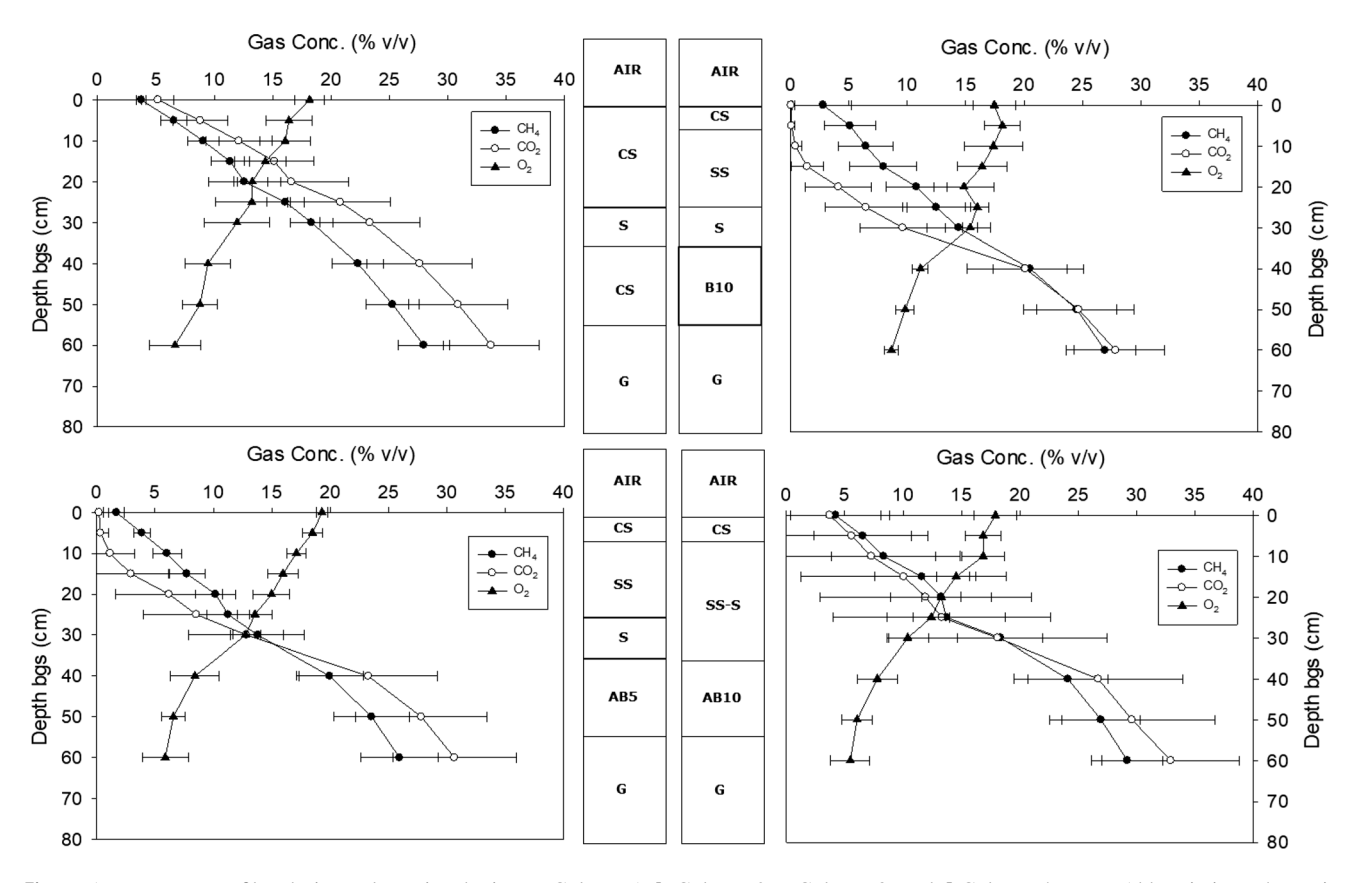


Fig. 3 Average gas profiles during column incubation: a Column 1; b Column 2; c Column 3; and d Column 4. Note: Abbreviations shown in Fig. 2

attributed to the reaction of H2S with heavy metal salts present in the paints. Hydrogen sulfide is also readily adsorbed on the soil surface or into the water in the soil pores and may get oxidized by the microorganisms [24, 25, 46]. In the study by Xia et al. [46],  $H_2S$  was absorbed completely in the bottommost part of the biocovers (landfill cover soil and waste biocover soil) and remained undetected in the middle and upper layer of the tested cover systems suggesting soil itself has significant H<sub>2</sub>S removal potential. In addition, BOF slag also has high H<sub>2</sub>S removal potential due to the presence of iron oxides [14]. Figure 4a shows headspace CH<sub>4</sub> concentrations in the four columns. All the cover systems showed significant reduction in the CH<sub>4</sub> emissions into the headspace, which could be attributed to the microbial CH<sub>4</sub> oxidation along with dilution. In column 1, headspace CH<sub>4</sub> concentrations remained relatively higher than other cover systems throughout the incubation period suggesting relatively lower microbial oxidation than biochar-amended soils. Columns with biochar-amended soils showed lower CH<sub>4</sub> emissions in general except for column 4, which showed occasional peaks in headspace CH<sub>4</sub> concentrations, which could be likely due to preferential flows due to potential desiccation cracking through underlying layers. Yargicoglu and Reddy [48] also reported such occasional high concentrations of gases in the headspace due to the preferential flows through cracks developed in the soil cover. Overall, column 3 showed lowest headspace CH<sub>4</sub> concentrations indicating highest microbial activity. It shows that the activated biochar helps to sustain microbial activities in the long term. The average CH<sub>4</sub> removal efficiencies (calculated based on the outlet and inlet CH<sub>4</sub> fluxes, [48] were 80%, 90%, 92% and 84% for column 1, column 2, column 3 and column 4, respectively (Fig. 4b). Figure 4c shows headspace CO<sub>2</sub> concentrations during the column operation period. Column 2 and column 3 that had SS media removed CO<sub>2</sub> completely throughout the operation period, whereas column 4 that had SS-S media underwent breakthrough after nearly 10 days of operation. On the other hand, column 1 showed consistently higher headspace CO<sub>2</sub> concentration. This shows that cover system with biocharamended soil and BOF slag can effectively mitigate CH<sub>4</sub>, CO<sub>2</sub> and H<sub>2</sub>S. The BOF slag in column 2 and column 3 did not undergo a complete breakthrough even after 36 days of CO<sub>2</sub> exposure and showed nearly 100% CO<sub>2</sub> removal (based on the inlet and outlet CO<sub>2</sub> fluxes, [48]) during the entire period of operation (Fig. 4d) showing significant potential in BOF slag for CO<sub>2</sub> removal under LFG



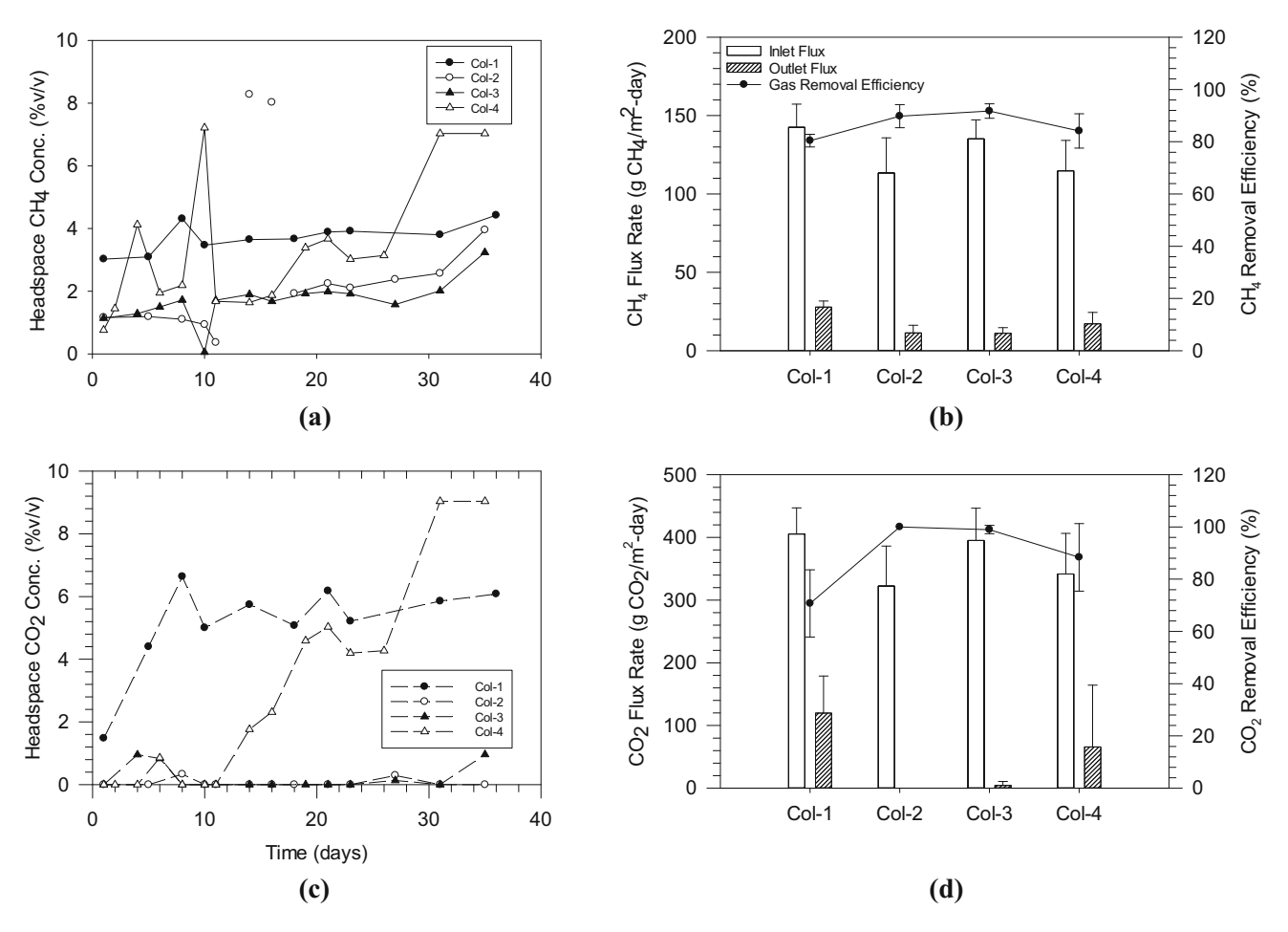


Fig. 4 a Concentration of CH4 in the headspace, **b** flux and removal efficiency of CH4, **c** concentration of CO2 in the headspace, and **d** flux and removal efficiency of CO2 during LFG exposure in the four column profiles

conditions. However, it is hard to interpret the exact CO<sub>2</sub> removal capacity of the BOF slag in the column setup as the CO<sub>2</sub> concentration gradients developed along the depths are the result of multiple phenomena such as diffusion, reaction, CH<sub>4</sub> oxidation, and gas flow making it hard to discern the contribution of each phenomenon [16]. For example, column 1, which did not have any BOF slag, also showed 70% average CO<sub>2</sub> removal (Fig. 4d), clearly indicating the contribution of processes other than carbonation reactions for reduction in headspace CO<sub>2</sub> concentration. Similarly, column 4 that had mixture of BOF slag and sand showed average CO<sub>2</sub> removal of 88%, which was lower than the BOF slag alone. Carbonate contents of the BOF slags from various depths were analyzed after column exhumation, and batch test was performed on carbonated slag from column 3 to estimate the amount of CO<sub>2</sub> removed by the BOF slag during column exposure.

# 3.3 Terminal methane oxidation rates

Methane oxidation rates were evaluated in batch tests for bottom biologic layer. Figure 5 shows the rate of headspace CH<sub>4</sub> concentration depletion for each bottom biologic sample. None of the samples showed lag phase and showed a rapid decline in CH<sub>4</sub> concentrations confirming microbial activity. The rate of CH<sub>4</sub> depletion was uniformly rapid in all AB5 subsamples (Fig. 5c) and AB10 mainly in the top (35–45 cm bgs) (Fig. 5d). The CH<sub>4</sub> depletion followed zero-order kinetics, which is consistent with previous studies [23, 48]. The CH<sub>4</sub> oxidation rates also were evaluated for the samples extracted from the top of each column and at various depths along the soil layer in column 1, which are shown in Fig. 6. Many studies have shown that the zone of maximum oxidation lies in the upper 15–30 cm of the cover system [16, 23, 30, 49] and is mainly attributed to higher aeration close to the surface of the cover system. On the contrary, in this study, the columns were fully aerated throughout the depth of the column (Fig. 3) and significant CH<sub>4</sub> oxidation occurred in the



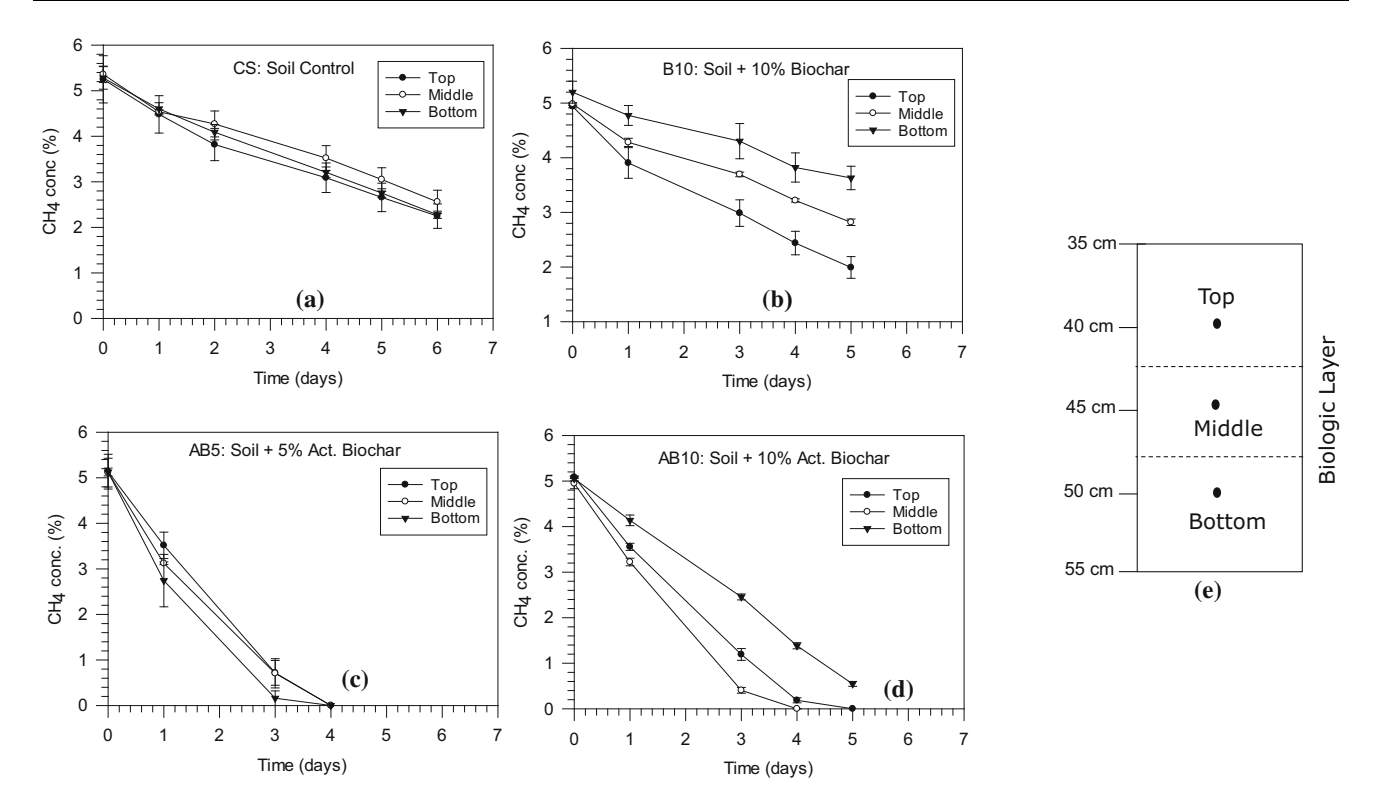


Fig. 5 Change in headspace CH4 concentrations with time during terminal batch testing on the exhumed samples from top, middle and bottom of each biologic layer in: a Column 1; b Column 2; c Column 3; and d Column 4; and e Schematic of biologic layer showing sample locations

biologic layers despite being situated at the deeper strata of the cover system (Fig. 6). Improved aeration and higher CH<sub>4</sub> oxidation could be associated with low bulk densities and high porosities of each layer in the column (Table 2) as studies have shown positive correlation between porosity (mainly air-filled porosity) and CH<sub>4</sub> oxidation rates in biocovers [30, 49]. Average CH<sub>4</sub> oxidation rates in AB5 and AB10 were 3 to 3.5 times more than that of CS and B10. A particular trend in CH<sub>4</sub> oxidation with depth could not be established in biologic layer as each sample showed different trends; for example, AB5 showed maximum CH<sub>4</sub> oxidation rate ( $\sim 145 \mu g/g$ -day) at the bottom (50 cm bgs) and lowest ( $\sim 130 \,\mu\text{g/g-day}$ ) at the middle (45 cm bgs), whereas AB10 showed maximum oxidation ( $\sim 134 \mu g/g$ day) at the middle and lowest ( $\sim 81 \,\mu g/g$ -day) at the bottom. Similarly, B10 showed maximum oxidation ( $\sim 50 \,\mu g/g$ -day) at the top (40 cm bgs) and lowest ( $\sim 28 \,\mu\text{g/g-day}$ ) at the bottom. CS had nearly similar CH<sub>4</sub> oxidation rates throughout the biologic layer (43, 39, and 43 μg/g-day at the top, middle, and bottom, respectively) as shown in Fig. 6. This suggests that there was more heterogeneity in the biochar-amended soil samples than soil control, resulting in variable microbial colonization and CH<sub>4</sub> oxidation rates. The CS media above sand layer in column 1 showed higher CH<sub>4</sub> oxidation rates than the bottom biologic layer, indicating that the upper regions were better aerated than the lower regions supporting better

microbial growth, which is consistent with previous studies [16, 23, 30]. Assuming that the upper horizons had better aeration and microbial activity, AB5 and AB10 still showed greater  $\mathrm{CH_4}$  oxidation rates than the topsoil region of column 1. This shows that the activated biochar-amended soils can sustain high microbial activity even in the lowermost aeration zones or facilitates aeration and microbial growth even at greater depths due to high internal porosity of biochar.

#### 3.4 Terminal material properties

The terminal MC, OC/LOI, and pH of the samples exhumed from variable depths of the column are summarized in Table 3. The bottom biologic layers in each column lost significant amount of moisture in the process of incubation under continuous gas flow conditions except for column 3, which lost only 2.3% compared to 6.7% (column 1), 5.3% (column 2) and 3.2% (column 4). The high microbial CH<sub>4</sub> oxidation in columns 3 and 4 could be the reason for relatively lower moisture loss, as water is produced during CH<sub>4</sub> oxidation [16]. Even though humidified air was supplied from the top of the column, drying of the layers could not be prevented due to the continuous synthetic LFG flow stripping away moisture from the soil pores. The bottom CS layer in column 1 showed the maximum loss in MC among all from initial 15% to



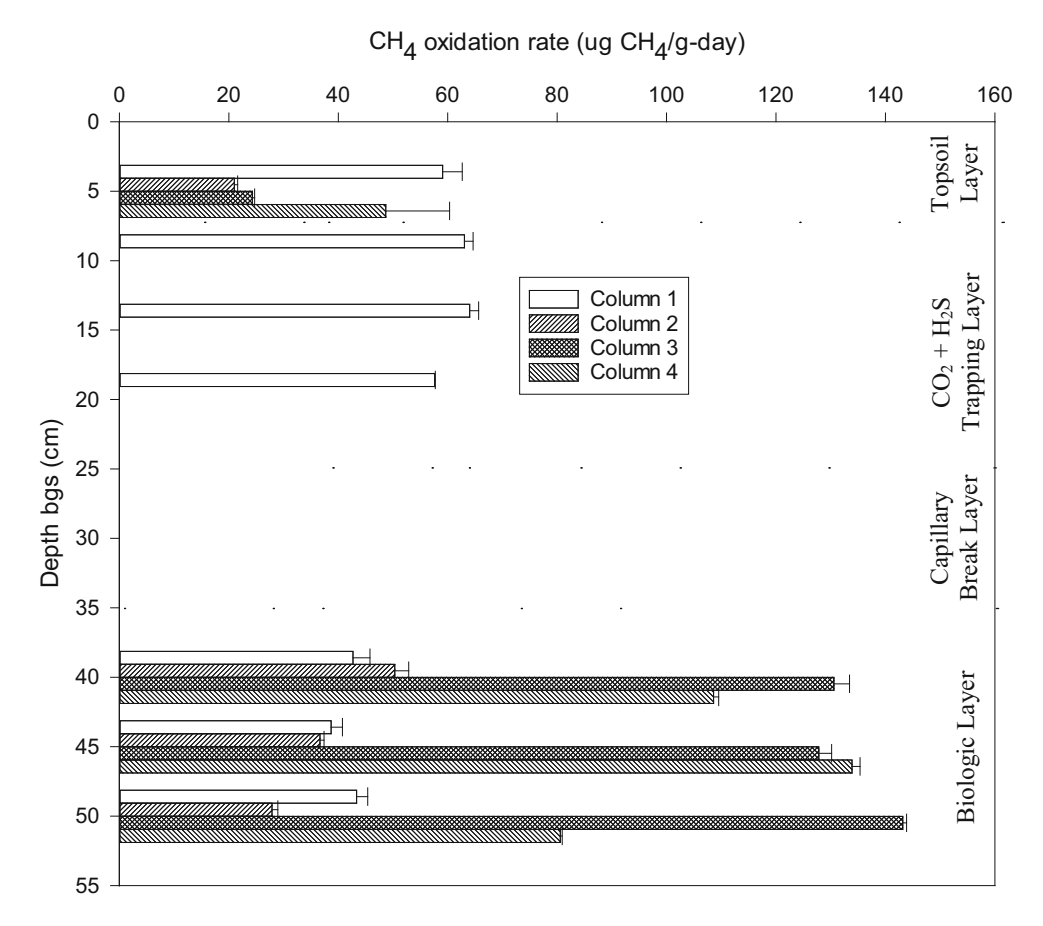


Fig. 6 Methane oxidation rates of the biologic layers at various depths of cover profile based on the batch incubation test. (Breaks denote different media)

average 8.4%. This drop in MC could be one of the reasons for lower CH<sub>4</sub> oxidation rates in terminal batch tests in CS as lower MC causes microbial stress resulting reduction in microbial activity [11, 12]. Biochar-amended soils also showed reduction in terminal MC; however, the reduction was not as significant as that of CS. The MC reduced to  $\sim 10\%$ , 12.5% and 12% in B10, AB5 and AB10, respectively. The activated biochar-amended soil samples (AB5 and AB10) retained more moisture than CS and B10 as biochar was soaked in methanotrophic culture during activation process and thus had more moisture held in the micropores. Biochar amendment prevented excessive loss of moisture due to high moisture absorption and retention abilities of biochar [50]. Organic content and pH of the soil samples remained nearly same as initial value except for AB10, which showed OC of 16.9% in the top (40 cm bgs). It could be from the deposition of microbial biomass and can be associated with the lower CH<sub>4</sub> oxidation rate in top (Fig. 6). The pH of the BOF slag reduced from 12.4 to a range of 10.6–11.9, which is associated with the carbonation reactions forming carbonate precipitates resulting in lowering of the pH [14, 44]. The SS-S media did not show significant drop in pH, which could be associated with low

carbonation reactions (Fig. 4b) and point to the presence of preferential flow paths. Loss on ignition increased slightly from 1.9 to 2.4 mainly in column 3, which could be associated with the deposition of carbonate precipitates from carbonation reactions.

Carbonation of the BOF slag led to hardening of the slag layer, which created hard mass-like weakly cemented sand making the exhumation process difficult. However, the carbonated mass was not hard like a rock and was brittle which broke easily upon hammering. Carbonate content tests were performed on the exhumed samples at various depths, as shown in Fig. 7. The virgin BOF slag had a very low carbonate content (0.04 g CaCO<sub>3</sub>) compared to other corresponding media. The pea gravel used in the gas distribution layer had a minimal carbonate content (0.04 g CaCO<sub>3</sub>), which rules out potential reaction of H<sub>2</sub>S with carbonates (in pea gravel) as a possible mechanism (Eq. 3) for H<sub>2</sub>S absorption.

$$CaCO_3 + H_2S = CaS + H_2O + CO_2$$
 (3)

The significant increase in the carbonate content in SS media in column 2 and column 3 confirms the removal of  $CO_2$  during column operation. Interestingly, carbonated SS



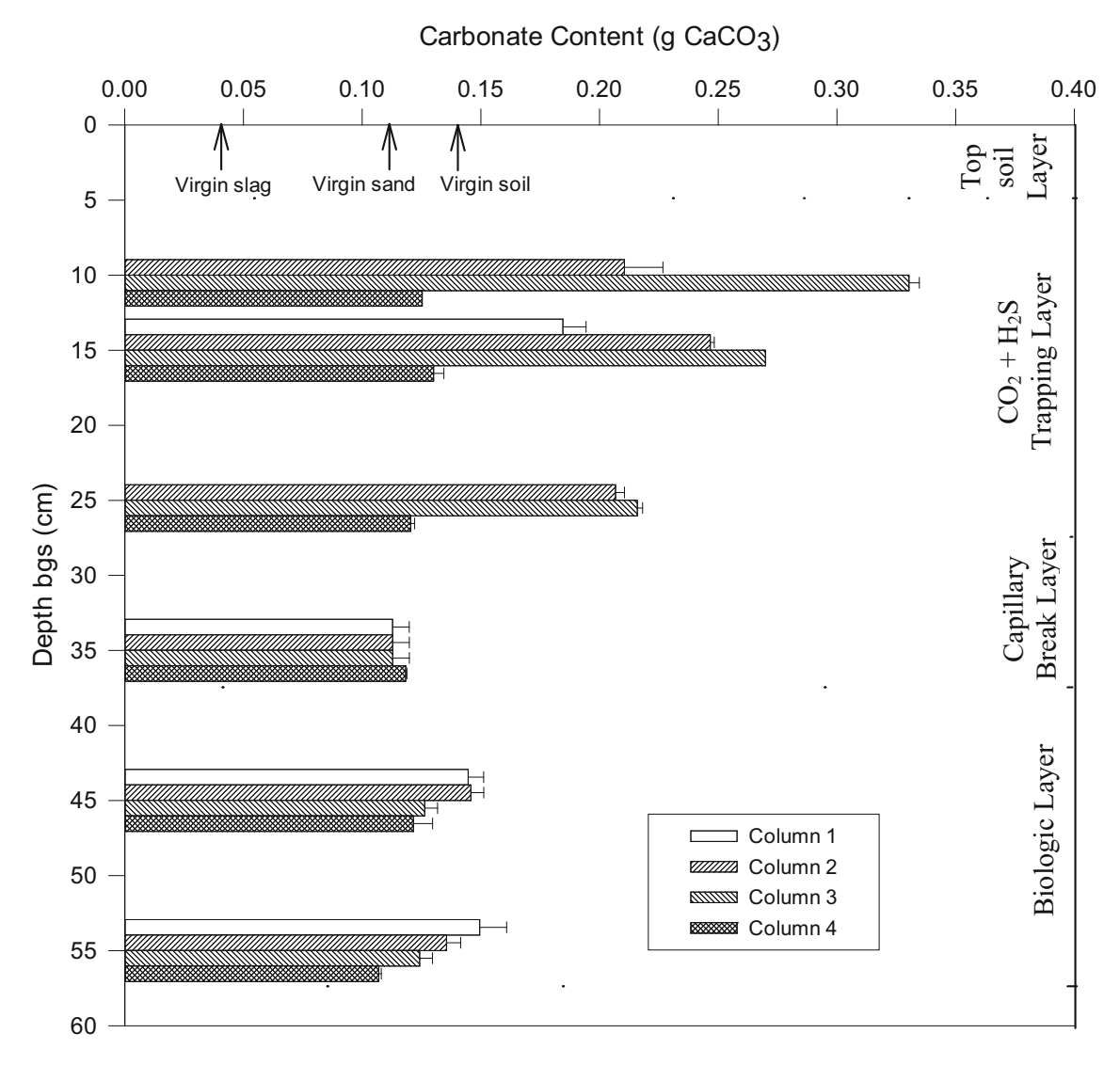


Fig. 7 Carbonate content of exhumed solids after testing

in column 2 showed slightly lower carbonate content than column 3 although both were initially from the same batch of the slag and had similar porosity and dry densities in the column. One plausible explanation is that the higher CH<sub>4</sub> oxidation rates of AB5 versus B10 enabled more CO2 sequestration (Fig. 3c). Another interesting observation was higher carbonate content in the upper part of the slag layers (Fig. 7), which was consistent with the reduction in pH (Table 3), although LFG was fed from the bottom of the column. One plausible reason could be due to the air fed from the top of the column, which also contained atmospheric CO<sub>2</sub> increasing the CO<sub>2</sub> load in the upper layers. Atmospheric aging is a commonly adopted technique to reduce volume instability/swelling of steel slags for aggregate application [27, 51]. The maximum carbonate content observed in the SS media in column 3 was 0.33 g CaCO<sub>3</sub>/g BOF slag at top 5 cm of the SS layer (10 cm

bgs), which corresponds to  $CO_2$  removal capacity of 145.2 mg  $CO_2/g$  BOF Slag. Similarly, the carbonate content at 20 cm of SS layer (25 cm bgs) was lower than the top and was 0.22 g  $CaCO_3/g$  BOF slag corresponding to 96.8 mg  $CO_2/g$  BOF slag. Hence, batch test was performed on the carbonated SS media from 20 cm depth (25 cm bgs) in column 3 to evaluate the residual carbonation capacity of the slag. The resultant residual carbonation capacity was  $\sim 37$  mg  $CO_2/g$  BOF slag (Fig. 8). Considering  $CO_2$  removal potential of BOF slag as 145.2 mg  $CO_2/g$  BOF slag, the 20-cm-thick slag layer can successfully remove  $CO_2$  for approximately 13 years assuming that  $CO_2$  emission rate is 4000 g $CO_2/m^2$ -year. It should be noted that the design life of the BOF slag in the cover varies with the  $CO_2$  flux rates prevalent at the site.

The carbonate content of carbonated SS-S media was marginally higher than virgin sand (Fig. 8) suggesting



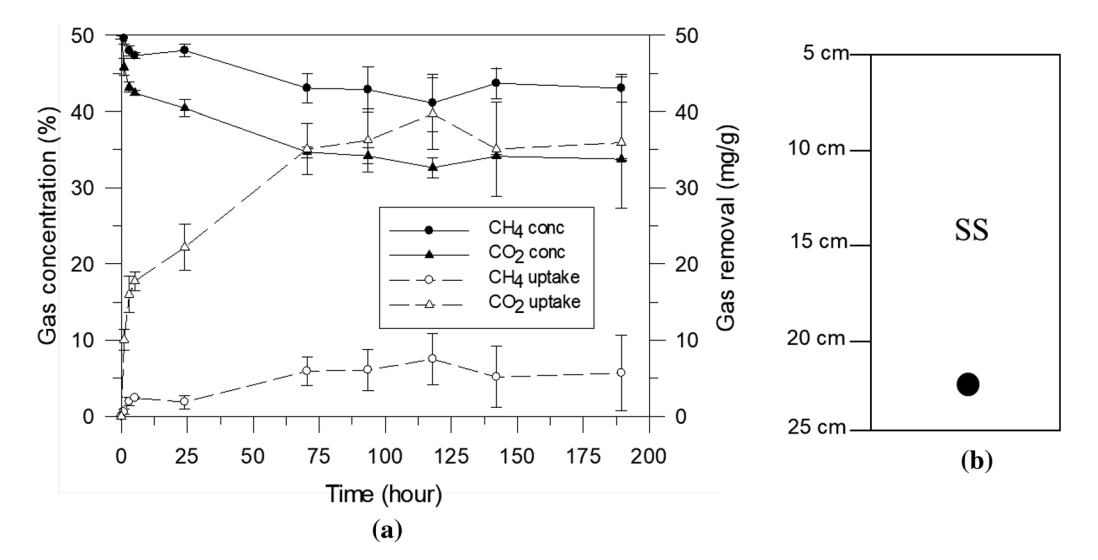
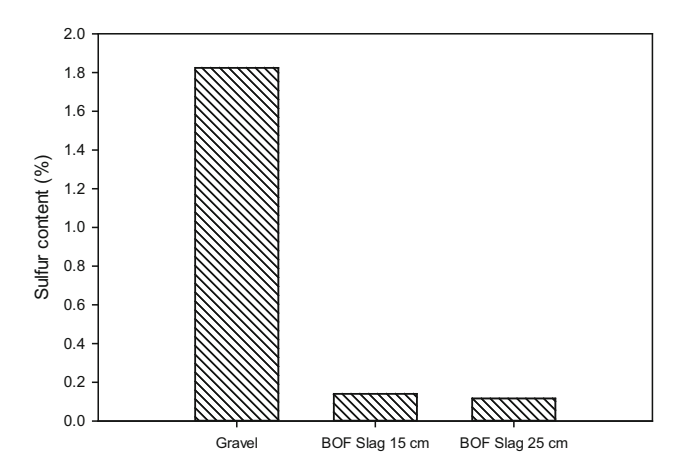


Fig. 8 a Residual CH4 and CO2 removal capacity of the BOF steel slag exhumed from the bottommost part (20–25 cm bgs) of the SS layer in column 3 and b) schematic representation of SS-S layer in the column

minimal carbonation reaction occurred in the mixture, which is again confirmed by minimal reduction in pH (Table 3). The reason for lower carbonation reaction in BOF slag upon mixing with sand is not clear as the system had same volume of slag as the other columns as well other parameters such as MC, bulk density, and porosity were kept consistent. Although the exact reasoning is not clear, one probable reason could be the presence of preferential flow paths in the layer reducing the residence time and carbonation reactions.

The sulfur content of the gravel and carbonated BOF slag taken from column 3 is shown in Fig. 9. The elevated sulfur content of gravel (1.8%) confirms that the significant amount of  $H_2S$  was removed in the GDL which protected the overlying layers from exposure to  $H_2S$ . The sulfur



**Fig. 9** Total sulfur content in the column exhumed gravel and BOF slag samples from column 3. Note: Gravel sample was taken from around the inflow gas port at the bottom of the column where darkening of gravel was concentrated

content of the carbonated BOF slag was significantly low (0.14-0.11%), which shows that the BOF slag was not exposed to H<sub>2</sub>S as BOF slag itself possesses significant H<sub>2</sub>S removal potential [14]. This indicates that the H<sub>2</sub>S removal potential of BOF slag could not be mobilized during the column operation.

## 3.5 SEM/EDS analysis

SEM/EDS analysis was performed on the carbonated SS and SS-S samples taken from the bottommost part of each column. The SS samples showed both heavily carbonated and less carbonated particles during scanning. Figure 10a shows SEM image of a heavily carbonated SS particle from column 2. The surface of the particle showed the formation of densely aggregated rhombohedral plate-like structures, which were identified as carbonate crystals packed densely due to prolonged carbonation [14, 26]. Although the surface showed densely packed carbonate crystals, the surface showed some pores (Fig. 10a) indicating potential gas flow paths. On the other hand, the less carbonated particles displayed rod-shaped structures with more porous surface (Fig. 10b), which were identified as unreacted portlandite [Ca(OH)<sub>2</sub>] and calcium silicates having a similar surface morphology to the virgin slag [14]. This could be the reason the carbonated SS media showed notable residual carbonation capacity during batch test (Fig. 8). The EDS spectrum confirms the formation of CaCO<sub>3</sub> based on calcium (Ca), carbon (C), and oxygen (O) (Fig. 11c). Similar to column 2, the carbonated SS media in column 3 also showed heavily carbonated particles with dense plate-like formations on the surface (Fig. 11a) and seemingly less carbonated particles (Fig. 11b) with EDS spectrum similar to column 2



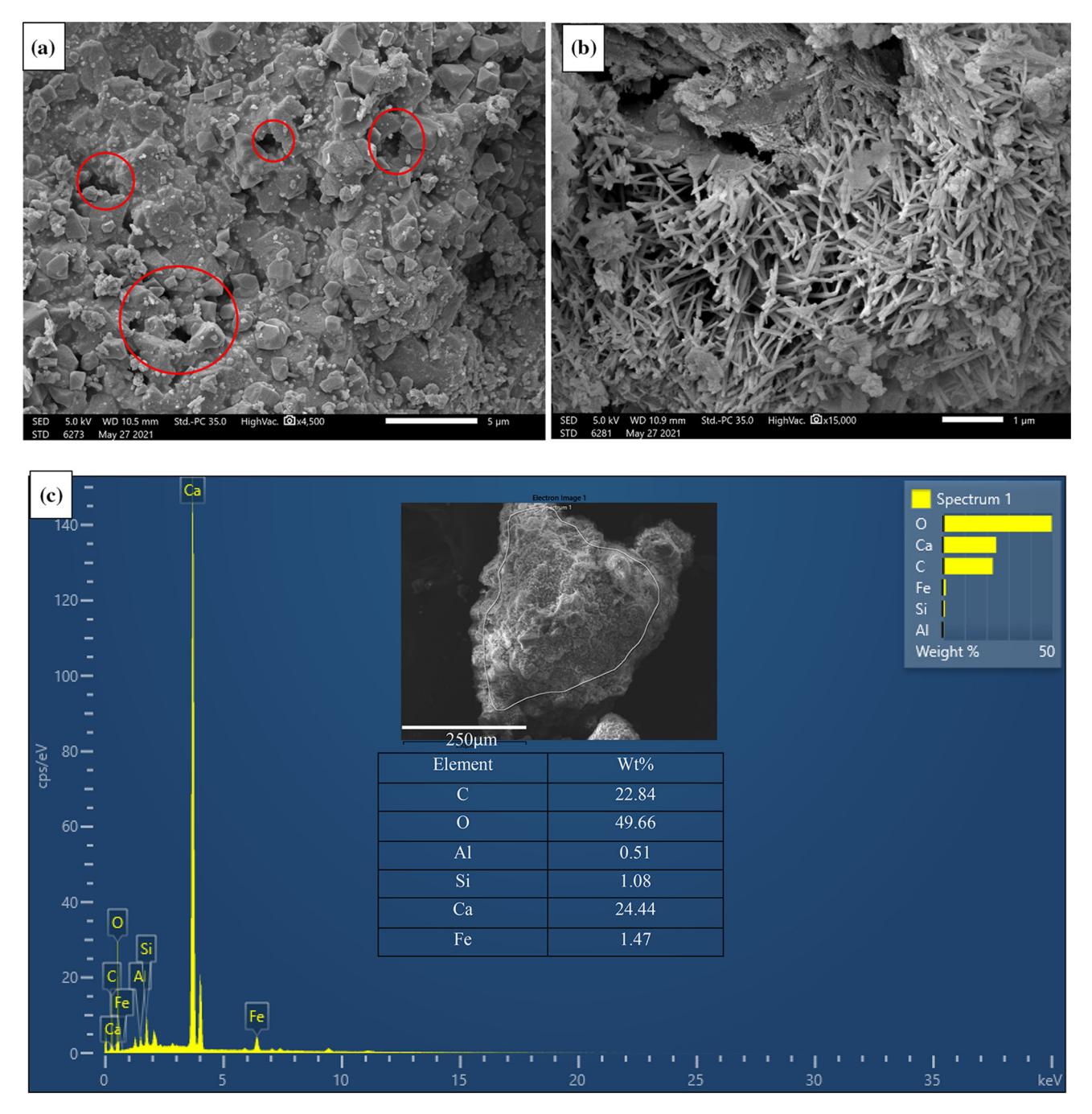


Fig. 10 Scanning electron micrographs of carbonated BOF slag from column 2; a heavily carbonated surface; b less carbonated surface; c EDS spectrum of one whole particle surface

(Fig. 11c). None of the EDS spectra showed the presence of sulfur (S), which indicates that H<sub>2</sub>S did not reach SS layer and was absorbed in the underlying gravel layer.

Figure 12a shows a carbonated SS-S media. The SS-S particle showed two distinct surfaces: 1) more undulated and 2) smoother surface (Fig. 12b). Similar transitional surfaces were reported by Jing et al. [22] during hydration of river sand and mortar cement stone. The enlarged image

of undulated surface showed highly porous surface filled with thin hexagonal plate-like structures which could be unreacted [Ca(OH)<sub>2</sub>] [29]. The smoother surface, on the other hand, was dense and appeared as a coating on the undulated surface as some flaky structures could be seen underneath the coating in some locations (Fig. 12c). This suggests that the BOF slag particle surfaces were likely blocked by the sand particles limiting CO<sub>2</sub> exposure and



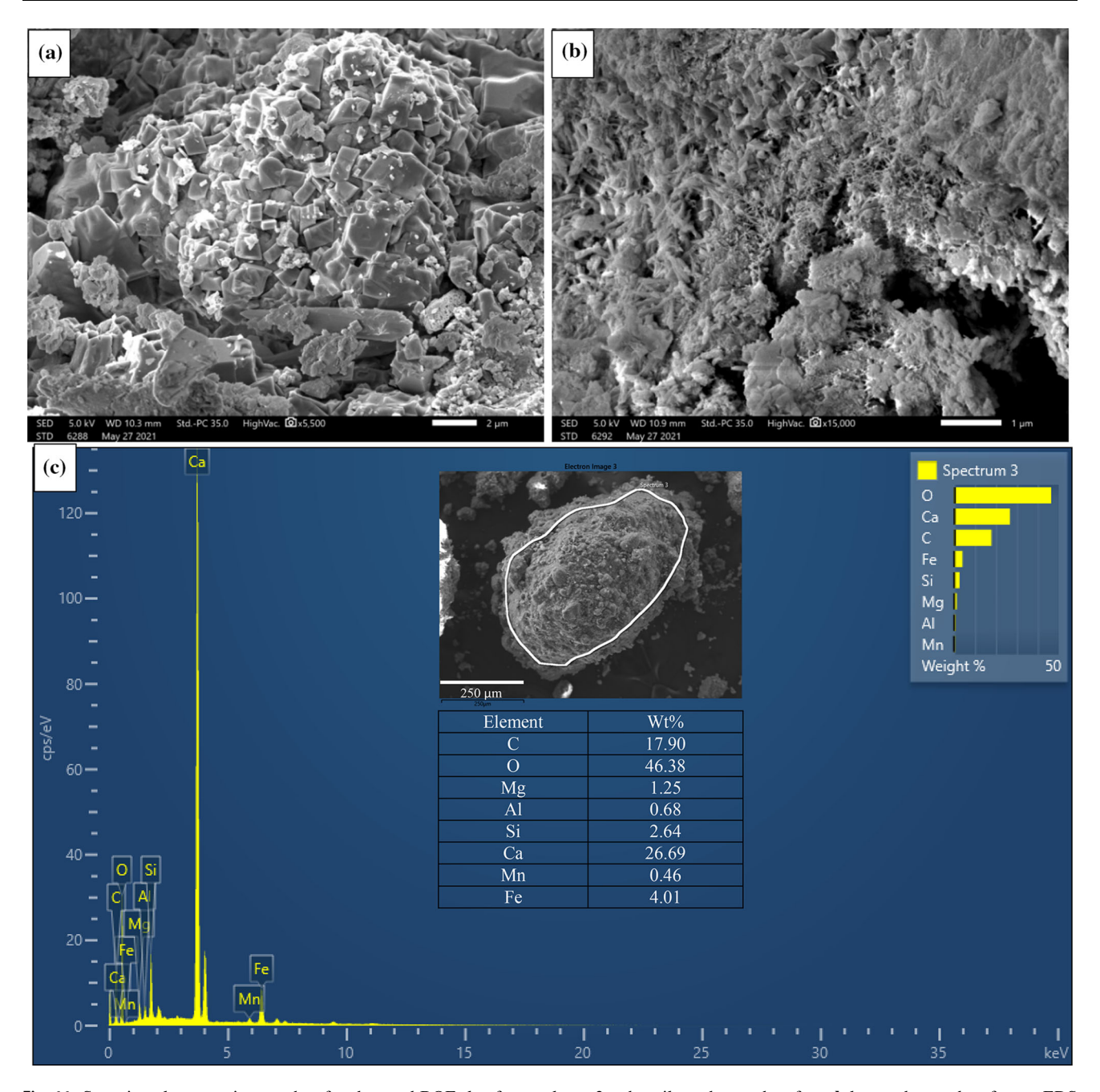


Fig. 11 Scanning electron micrographs of carbonated BOF slag from column 3; a heavily carbonated surface; b less carbonated surface; c EDS spectrum of one whole particle surface

carbonation reactions. Overall, the morphology of the carbonated BOF slag suggested that the carbonation process does not completely block the surface pores and hinder the gas flow conditions.

Overall, the column study showed that the activated biochar-amended soil can sustain microbial activity irrespective of the location in the cover system. The presence of highly alkaline BOF slag layer over biologic layer does not endanger the oxygen intrusion into the underlying biologic layer. However, these observations need to be verified with

field-scale studies. In addition, one of the limitations of this study is the duration of the column operation. After addition of BOF slag layer, the column was only operated for 36 days due to the onset of global pandemic and sudden lockdowns of the facilities. As a result, the BOF slag did not undergo a complete breakthrough and effect of slag carbonation on the gas flow could not be evaluated in detail. Hence, further study is warranted to capture this effect to derive conclusive remarks. In addition, since most of the  $\rm H_2S$  was absorbed in the gravel layer, the effect of  $\rm H_2S$  on



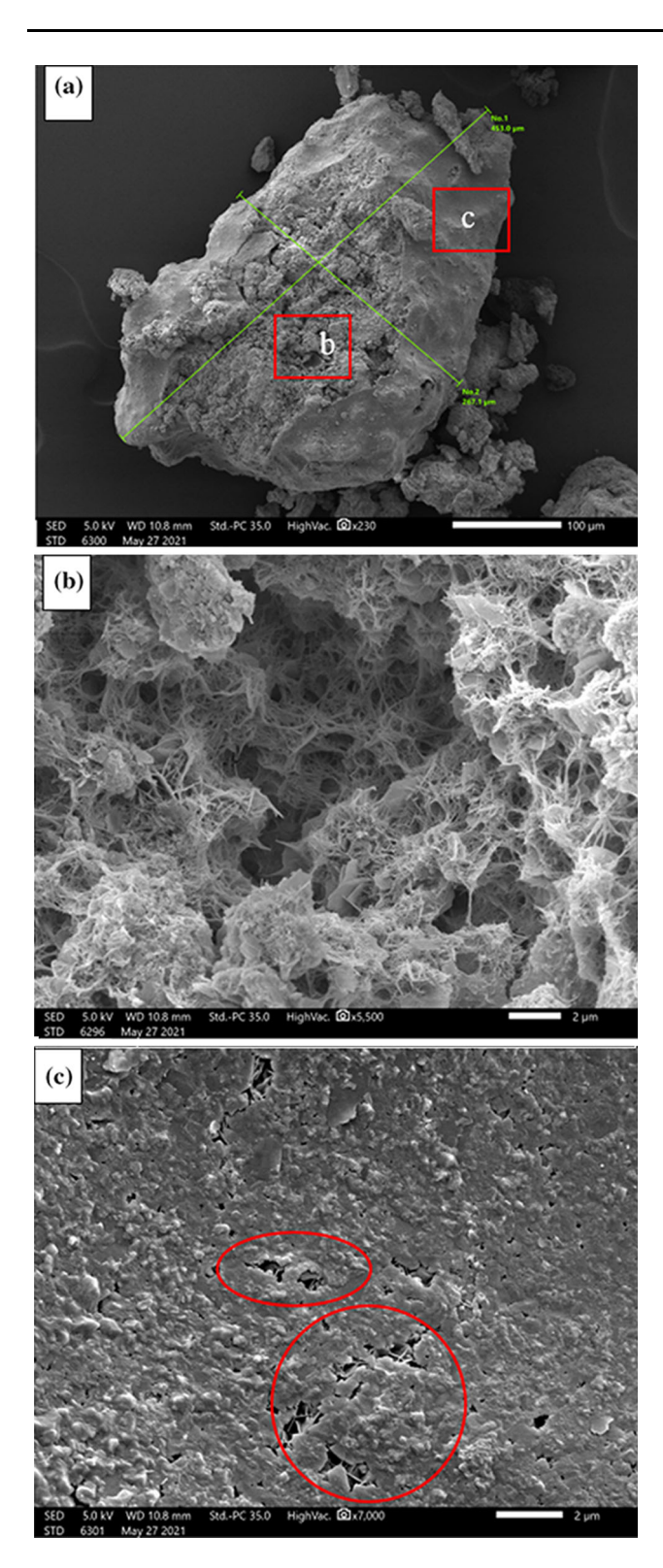


**Fig. 12** Scanning electron micrographs of carbonated SS-S media from column 4; **a** micrograph of carbonated SS-S particle; **b** enlarged image of SS-S media at location "b"; **c** enlarged image of SS-S media at location "c"

microbial activity of the overlying biological layer was not reflected in this study. Hence, further study is needed to delineate the effect of  $H_2S$  on the microbial  $CH_4$  oxidation in the biologic layer.

## 4 Conclusions

Three different biogeochemical covers and soil control cover systems were used to treat simulated LFG containing mixture of 48.25% CH<sub>4</sub>, 50% CO<sub>2</sub> and 1.75% H<sub>2</sub>S at an inflow flux of 130 g CH<sub>4</sub>/m<sup>2</sup>-day. The addition of BOF slag layer above biologically active layer significantly reduced the fugitive emissions of CO<sub>2</sub> and H<sub>2</sub>S in addition to CH<sub>4</sub>, where biochar-amended soil and BOF slag systems (column 2 and column 3) showed 90–94% CH<sub>4</sub>, 100% CO<sub>2</sub> and 100% H<sub>2</sub>S removal during column incubation period. Biochar activation with methanotrophic bacterial consortium reduced the initial lag phase and increased the CH<sub>4</sub> oxidation at amendment ratios as low as 5% (143 µg CH<sub>4</sub>/ g-day). BOF slag positioned over top of soil cover system did not hamper oxygen flow into the underlying biologic layer or affect the performance of the biologic layer. Since H<sub>2</sub>S was absorbed in the underlying gravel layer, before reaching the BOF slag layer, H<sub>2</sub>S removal potential of slag was not mobilized during the column operation. Carbonation of BOF also did not affect the gas flow within the cover system. SEM imaging further confirmed that carbonation does not turn slag into impervious hard mass and impede gas flow. Overall, biogeochemical cover offers a sustainable solution for mitigation of fugitive LFG emissions and valorization of waste materials like steel slag and waste biomass in the form of biochar.

Acknowledgements This research is a part of comprehensive project titled "Innovative Biochar-Slag-Soil Cover System for Zero Emissions at Landfills" funded by the National Science Foundation (CMMI# 1724773), which is gratefully acknowledged. Any opinions, findings, conclusions, and recommendations expressed in this material are those of the authors and do not necessarily reflect the views of the NSF. The authors are grateful to Electron Microscopy Center at the University of Illinois at Chicago for conducting SEM/EDS analysis and Phoenix Services, LLC, for providing BOF slag for this study. Authors are also grateful to Pittsburgh Mineral & Environmental Technology, Inc., for performing sulfur analysis on the column exhumed samples.

#### References

 ASTM D2434-19 (2019) Standard test method for permeability of granular soils (constant head). ASTM International, West Conshohocken



- ASTM D2487-17e1 (2017) Standard practice for classification of soils for engineering purposes (unified soil classification system).
   ASTM International, West Conshohocken
- ASTM D2974-20e1 (2020) Standard test methods for determining the water (moisture) content, ash content, and organic material of peat and other organic soils. ASTM International, West Conshohocken
- ASTM D2980-17e1 (2017) Standard test method for saturated density, moisture-holding capacity, and porosity of saturated peat materials. ASTM International, West Conshohocken
- ASTM D4318-17e1 (2017) Standard test methods for liquid limit, plastic limit, and plasticity index of soils. ASTM International, West Conshohocken
- ASTM D4373-14 (2014) Standard test method for rapid determination of carbonate content of soils. ASTM International, West Conshohocken
- ASTM D4972-19 (2019) Standard test methods for pH of soils.
  ASTM International, West Conshohocken
- ASTM D5084-16a (2016) Standard test methods for measurement of hydraulic conductivity of saturated porous materials using a flexible wall permeameter. ASTM International, West Conshohocken
- ASTM D6913 / D6913M-17 (2017) Standard test methods for particle-size distribution (gradation) of soils using sieve analysis. ASTM International, West Conshohocken
- ASTM D854-14 (2014) Standard test methods for specific gravity of soil solids by water pycnometer. ASTM International, West Conshohocken
- Boeckx P, Van Cleemput O (1996) Methane oxidation in a neutral landfill cover soil: influence of moisture content, temperature, and nitrogen-turnover. Am Soc Agron Crop Sci Soc Am Soil Sci Soc Am 25(1):178–183
- Chetri JK, Reddy KR (2021) Climate-resilient biogeochemical cover for waste containment systems. Geo-Extreme 2021: Climatic Extremes and Earthquake Modeling, ASCE Press, pp 189–199
- Chetri JK, Reddy KR, Grubb DG (2019) Innovative biogeochemical cover to mitigate landfill gas emissions: investigation of controlling parameters based on batch and column experiments. Environ Process 6(4):935–949
- Chetri JK, Reddy KR, Grubb DG (2020) Carbon-dioxide and hydrogen-sulfide removal from simulated landfill gas using steel slag. J Environ Eng 146(12):04020139
- Chetri JK, Reddy KR, Green SJ (2021) Methane oxidation and microbial community dynamics in activated biochar amended landfill soil cover. J Environ Eng. https://doi.org/10.1061/ (ASCE)EE.1943-7870.0001984
- De Visscher A, Thomas D, Boeckx P, Van Cleemput O (1999) Methane oxidation in simulated landfill cover soil environments. Environ Sci Technol 33(11):1854–1859
- Huang D, Yang L, Ko JH, Xu Q (2019) Comparison of the methane-oxidizing capacity of landfill cover soil amended with biochar produced using different pyrolysis temperatures. Sci Total Environ 693:133594
- Huber-Humer M, Gebert J, Hilger H (2008) Biotic systems to mitigate landfill methane emissions. Waste Manag Res 26(1):33–46
- Huber-Humer M, Tintner J, Böhm K, Lechner P (2011) Scrutinizing compost properties and their impact on methane oxidation efficiency. Waste Manag 31(5):871–883
- 20. Huijgen WJ, Witkamp GJ, Comans RN (2005) Mineral  $\rm CO_2$  sequestration by steel slag carbonation. Environ Sci Tchnol 39(24):9676-9682
- 21. IPCC (2014) Climate Change 2014: Synthesis Report. Contribution of working groups I, II and III to the fifth assessment report of the intergovernmental panel on climate change. In: Core

- Writing Team, R.K. Pachauri and L.A. Meyer (eds.). IPCC, Geneva, Switzerland, pp. 151
- Jing W, Jiang J, Ding S, Duan P (2020) Hydration and microstructure of steel slag as cementitious material and fine aggregate in mortar. Molecules 25(19):4456
- Kightley D, Nedwell DB, Cooper M (1995) Capacity for methane oxidation in landfill cover soils measured in laboratory-scale soil microcosms. Appl Environ Microbiol 61(2):592
- Lee EH, Moon KE, Cho KS (2017) Long-term performance and bacterial community dynamics in biocovers for mitigating methane and malodorous gases. J Biotechnol 242:1–10
- Lee YY, Jung H, Ryu HW, Oh KC, Jeon JM, Cho KS (2018) Seasonal characteristics of odor and methane mitigation and the bacterial community dynamics in an on-site biocover at a sanitary landfill. Waste Manag 71:277–286
- Mo L, Zhang F, Deng M (2016) Mechanical performance and microstructure of the calcium carbonate binders produced by carbonating steel slag paste under CO<sub>2</sub> curing. Cem Concr Res 88:217–226
- Motz H, Geiseler J (2001) Products of steel slags an opportunity to save natural resources. Waste Manag 21(3):285–293
- OSHA (2021) Hydrogen Sulfide. Occupational safety and health administration. United States Department of Labor. Available on https://www.osha.gov/hydrogen-sulfide/hazards (accessed on June 14, 2021)
- Pang B, Zhou Z, Xu H (2015) Utilization of carbonated and granulated steel slag aggregate in concrete. Constr Build Mater 84:454–467
- Rachor I, Gebert J, Gröngröft A, Pfeiffer EM (2011) Assessment of the methane oxidation capacity of compacted soils intended for use as landfill cover materials. Waste Manag 31(5):833–842
- Rai RK, Chetri JK, Reddy KR (2019) Effect of methanotrophicactivated biochar-amended soil in mitigating CH<sub>4</sub> emissions from landfills. In: Proceeding 4th international conference on civil and environmental geology and mining engineering, Trabzon, Turkey
- Reddy KR, Kumar G, Gopakumar A, Rai RK, Grubb DG (2018)
  CO<sub>2</sub> Sequestration using BOF slag: application in landfill cover.
  In International conference on protection and restoration of the environment XIV, Thessaloniki, Greece
- Reddy KR, Grubb DG, Kumar G (2018) Innovative biogeochemical soil cover to mitigate landfill gas emissions. In: International conference on protection and restoration of the environment XIV, Thessaloniki, Greece
- Reddy KR, Yargicoglu EN, Yue D, Yaghoubi P (2014) Enhanced microbial methane oxidation in landfill cover soil amended with biochar. J Geotech Geoenviron Eng 140(9):04014047
- Reddy KR, Rai RK, Green SJ, Chetri JK (2019) Effect of temperature on methane oxidation and community composition in landfill cover soil. Ind Microbiol Biotechnol 46(9–10):1283–1295
- Reddy KR, Chetri JK, Kumar G, Grubb DG (2019) Effect of basic oxygen furnace slag type on carbon dioxide sequestration from landfill gas emissions. Waste Manag 85:425–436
- Reddy KR, Gopakumar A, Chetri JK, Kumar G, Grubb DG (2019) Sequestration of landfill gas emissions using basic oxygen furnace slag: effects of moisture content and humid gas flow conditions. J Environ Eng 145(7):04019033
- 38. Reddy KR, Gopakumar A, Rai RK, Kumar G, Chetri JK, Grubb DG (2019) Effect of basic oxygen furnace slag particle size on sequestration of carbon dioxide from landfill gas. Waste Manag Res 37(5):469–477
- Sadasivam BY, Reddy KR (2015) Influence of physico-chemical properties of different biochars on landfill methane adsorption. In: IFCEE 2015, pp. 2647–2656
- Sadasivam BY, Reddy KR (2014) Landfill methane oxidation in soil and bio-based cover systems: a review. Rev Environ Sci Biotechnol 13(1):79–107



- Sadasivam BY, Reddy KR (2015) Adsorption and transport of methane in biochars derived from waste wood. Waste Manag 43:218–229
- Schuetz C, Bogner J, Chanton J, Blake D, Morcet M, Kjeldsen P (2003) Comparative oxidation and net emissions of methane and selected non-methane organic compounds in landfill cover soils. Environ Sci Technol 37(22):5150–5158
- USEPA (2021) Basic information about landfill gas. Landfill methane outreach program (LMOP). United States environmental protection agency, Washington, DC, USA. Available on https:// www.epa.gov/lmop/basic-information-about-landfill-gas (Accessed on June 11, 2021)
- 44. van Zomeren A, Van der Laan SR, Kobesen HB, Huijgen WJ, Comans RN (2011) Changes in mineralogical and leaching properties of converter steel slag resulting from accelerated carbonation at low CO<sub>2</sub> pressure. Waste Manag 31(11):2236–2244
- 45. Wohlers HC, Feldstein M (1966) Hydrogen sulfide darkening of exterior paint. J Air Pollut Control Assoc 16(1):19–21
- Xia FF, Zhang HT, Wei XM, Su Y, He R (2015) Characterization of H<sub>2</sub>S removal and microbial community in landfill cover soils. Environ Sci Pollut Res 22(23):18906–18917
- 47. Xie T, Reddy KR, Wang C, Yargicoglu EN, Spokas K (2015) Characteristics and applications of biochar for environmental

- remediation: a review. Crit Rev Environ Sci Technol 45(9):939–969
- Yargicoglu EN, Reddy KR (2017) Effects of biochar and wood pellets amendments added to landfill cover soil on microbial methane oxidation: a laboratory column study. J Environ Manag 193:19–31
- Yargicoglu EN, Reddy KR (2018) Biochar-amended soil cover for microbial methane oxidation: effect of biochar amendment ratio and cover profile. J Geotech Geoenviron Eng 144(3):04017123
- Yargicoglu EN, Sadasivam BY, Reddy KR, Spokas K (2015)
  Physical and chemical characterization of waste wood derived biochars. Waste Manag 36:256–268
- 51. Yildirim IZ, Prezzi M (2009) Use of steel slag in subgrade applications. Joint transportation research program. Project No. C-36-50BB. Indiana Department of Transportation and The U.S. Department of Transportation Federal Highway Administration

**Publisher's Note** Springer Nature remains neutral with regard to jurisdictional claims in published maps and institutional affiliations.

